Barium adsorption on the chemisorbed O(2 × 1)/Ni(110) surface

2009 J. Phys.: Condens. Matter 21 445004

(http://iopscience.iop.org/0953-8984/21/44/445004)

J. Phys.: Condens. Matter **21** (2009) 445004 (6pp) doi:10.1088/0953-8984/21/44/445004

Barium adsorption on the chemisorbed O(2 × 1)/Ni(110) surface

Dimitrios Vlachos[1], **Stylianos D Foulias and Mattheos Kamaratos**

Department of Physics, University of Ioannina, PO Box 1186, GR-45110, Ioannina, Epirus, Greece

E-mail: dvlachos@cc.uoi.gr

Received 26 June 2009, in final form 11 September 2009
Published 9 October 2009
Online at stacks.iop.org/JPhysCM/21/445004

Abstract

Barium adsorption on the O(2 × 1)/Ni(110) surface has been studied by Auger electron spectroscopy and work function measurements in combination with photoemission measurements. The study was focused on the low coverage regime from submonolayer to double monolayer. The results show that during development of the first layer of Ba on the surface, a two-dimensional incomplete barium oxide layer, BaO, forms. This BaO layer is interspersed by Ba chemisorbed atoms reacting directly with Ni atoms. As the second layer of Ba is completed, the adsorbate approaches the metallic phase due to the Ba–Ba interaction. The low energy Auger transition lines of Ba (75 eV) and BaO (68 eV) shift towards lower energies as the Ba coverage increases. Previous photoemission measurements by synchrotron radiation are used to interpret these energy shifts, which are closely related to the barium oxidation process on the surface. The analysis shows the importance of the extra-atomic relaxation energy due to (1) the polarization of the O^{2-} anions from BaO and (2) the screening from the electron density at the Fermi level of the barium overlayer and the nickel substrate.

1. Introduction

The chemical interaction between metal adsorbates and oxygen on surfaces results in the development of surface oxides with different electronic, chemical and mechanical properties than those of the bulk oxides. Because of these properties, the oxidation of metal surfaces, and more generally the metal/oxide interfaces, have a large technological impact and numerous applications in materials science, microelectronics and chemistry. For example, thin oxide films are used in solid state devices (tunneling junctions, Schottky barrier junctions and Josephson tunnel devices), in magnetoelectronics, in heterogeneous catalysis, in surface passivation for natural corrosion protection, etc [1–3].

Among the metal oxides, barium oxide (BaO) is quite an important material in modern technology, mainly because of its low work function, electron emissivity and its catalytic [4] and superconducting properties [5]. In particular, the formation of BaO ultra-thin films on surfaces is of specific interest. Such films of BaO on metallic substrates of W and Pt, have given significant industrial applications in the fabrication of high current density cathodes [6, 7] and in the design of modern catalysts for NO_x compound storage in exhaust emission systems from motor vehicles [8–11].

To better understand the electronic and physicochemical properties of the BaO/substrate, it is important to study how the BaO overlayer starts developing on the surface from the submonolayer to the monolayer regime. Also, it is crucial to elucidate the nature of the bonding between Ba and O atoms when BaO forms on a surface. This is a controversial issue in the literature. For example, the simple electrostatic model, where the electropositive atom of Ba donates electrons to the electronegative O atom, cannot explain the negative binding energy shifts (NBES) of the barium atomic levels, which have been repeatedly observed by numerous experiments in BaO formation [4, 12–19]. Similar NBES have been measured for oxidation of Cs as well [20, 21]. So far, different explanations have been given for these unexpected energy shifts based on relaxation effects [13], changes in the final state screening [14], the Madelung potential [20, 21] and changes in the position of the Fermi level in the energy gap of the oxide [15]. Wertheim also explained the NBES by electron transfer from the delocalized 6s into the localized 5d atomic states during the formation of BaO [22]. On the other hand, Parmigiani and his colleagues [23, 24], studying theoretically

[1] Author to whom any correspondence should be addressed.

cluster model wavefunctions for the alkaline-earth oxides, showed that the Madelung potential arising from the existence of an ionic crystal is responsible for the NBES. Vasquez has also argued that changes in the Madelung potential and the work function of the surface upon oxidation can interpret the NBES [16]. From the above, it is clear that there are a number of factors resulting in these peculiar observed NBES of the cation atomic levels. In our recent work [25], we studied the NBES for BaO formation by adsorbing oxygen on a bariated Ni(110) surface. In that work, x-ray photoemission spectroscopy (XPS) measurements of Ba 4d, 5s and 5p core levels combined with previous AES results indicated that initial (Madelung potential) and final state effects (extra-atomic relaxation) contribute to the NBES [25].

In the present work we study the oxidation of barium by adsorbing Ba on the chemisorbed O(2 × 1)/Ni(110) surface. This is a rather unusual process of developing BaO on a surface, since the more common way is either by oxidizing a bariated surface [7, 15, 26, 27] or by directly using a BaO evaporation source [28–30]. However, we believe that by adsorbing Ba on an oxygen pre-covered surface, we expect a new insight into the Ba–O interaction mechanism. Indeed, in a recent paper [31], we deposited Ba on a fully oxidized Ni(110) surface resulting in BaO by the reduction of the substrate oxide. In that work the measured Auger electron energy shifts (AEES) were negative and were interpreted by the extra-atomic relaxation effects due to the highly polarizable O^{2-} anions. In this work we mostly focus on the low energy (<100 eV) Auger electron transition lines of Ba and BaO, since the emitted electrons are valence band electrons carrying valuable information about the Ba–O bonding. In addition, the Ba and BaO Auger transition lines are closely related to the atomic levels that show significant binding energy shifts in the photoemission experiments. The results show that the low energy Ba and BaO Auger lines move also towards lower energies. One of the purposes of this work is to explain the physical origins of the AEES and how relevant these are to the barium oxidation process. To succeed in this, we use some previously measured Ba core atomic and valence band photoemission spectra obtained by synchrotron radiation facilities [25].

2. Experimental part

All the measurements were performed in an ultra-high vacuum system (UHV) at a base pressure of 10^{-10} Torr. The system was equipped with Auger electron spectroscopy (AES), low energy electron diffraction (LEED), a quadrupole mass spectrometer and a Kelvin probe for work function (WF) measurements. The substrate was a Ni(110) single crystal with dimensions 1 cm × 0.5 cm × 0.1 cm mounted on a X–Y–Z manipulator. The crystal could be heated to 750 °C by a Ta tape firmly attached at the back side of the crystal, and uniformly pressed between the crystal and a Ta metallic case. The temperature of the Ni crystal could be measured by a NiCr–CrAl thermocouple spot-welded onto the center of the Ta case and calibrated by an infrared pyrometer in the 600–900 °C range. The deposition of Ba was done by using a commercial evaporation SAES Getters source at constant current 6.5 A in steps of 2 min deposition time. Assuming that the sticking coefficient of Ba on the oxygen predeposited nickel is constant and equal to that on the clean surface, the coverage could be estimated in monolayers (∼0.05 ML min^{-1}) by combining previous AES, LEED, TDS and WF results [32]. For the cleaning of the Ni crystal, an argon ion gun was used for sputtering at an energy $E = 2$ keV, partial pressure $P_{Ar} \sim 5 \times 10^{-5}$ Torr and sputtering time $t \sim 20$ min. After the sputtering process and a following annealing at 400 °C, a sharp 1 × 1 LEED pattern of the Ni(110) surface could be observed. The oxygen adsorption on the nickel surface took place by supplying molecular oxygen of purity 99.998 vol% into the experimental chamber through a leak valve. The oxygen exposure was measured in Langmuirs (L), where 1 L = 1×10^{-6} Torr s.

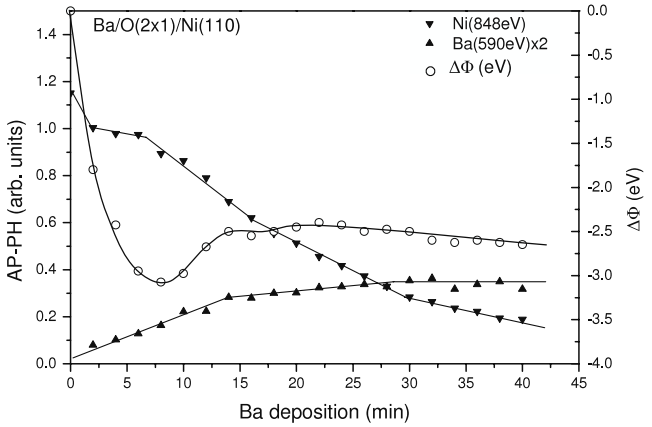

Figure 1. The AP-PH of the Ba (590 eV) and Ni (848 eV) Auger transition lines and the WF change, ΔΦ, for Ba deposition on the oxygen chemisorbed O(2 × 1)/Ni(110) surface.

The AES measurements were performed by utilizing a primary electron beam with energy $E = 2$ keV. The Auger electrons were collected and analyzed by a Varian cylindrical mirror analyzer (CMA), with an accuracy of 0.1 eV for the O(KLL) Auger transition line. The AES spectra were recorded in the first derivative mode, $dN(E)/dE$, and the intensity was measured from the peak-to-peak height (AP-PH). By convention the energy of an Auger electron transition line was defined at the high energy wing of the differentiated peaks. The WF measurements were taken by the Kelvin probe with an accuracy of 0.02 eV.

3. Results and discussion

3.1. AES and WF results

The first step was to form the oxygen chemisorbed phase O(2 × 1)/Ni(110) surface by exposing the nickel surface to ∼2 L of oxygen. This is the initial adsorption stage of oxygen on the Ni(110) surface [33].

Then we started the Ba deposition on the oxygenated nickel surface. Figure 1 shows the measured AP-PH for the Ba (590 eV) and Ni (848 eV) Auger transition lines as well as the change of the induced work function, ΔΦ. Clearly,

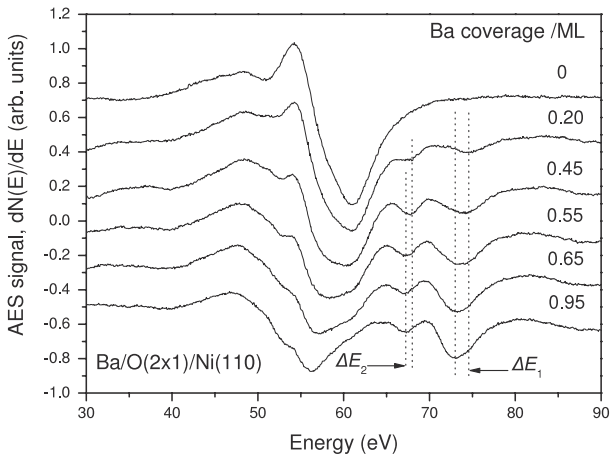

Figure 2. The low energy AES spectra for Ba adsorption on the O(2 × 1)/Ni(110) surface are shown for different barium coverages. Note the energy shifts ΔE_1 and ΔE_2 of the Ba (75 eV) and BaO (68 eV) Auger transition lines, respectively (indicated by the dotted vertical lines), as the Ba coverage grows.

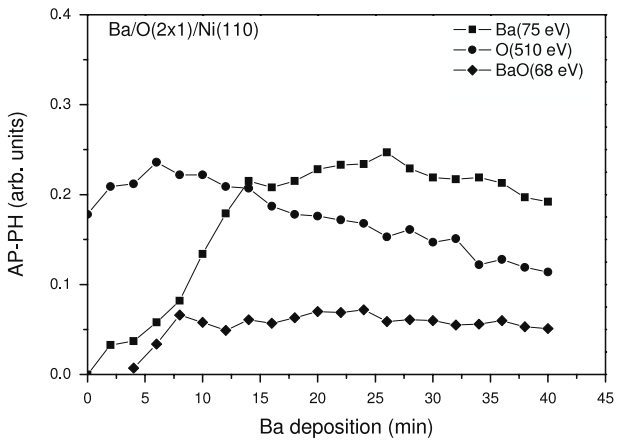

Figure 3. The AP-PH of the Ba (75 eV), BaO (68 eV) and O (510 eV) Auger transition lines as a function of the barium deposition time on the oxygen chemisorbed O(2 × 1)/Ni(110) surface.

a linear increase of the Ba (590 eV) line occurs with the change of slope at periodic deposition time intervals (14 and 28 min, respectively). In parallel, an almost linear decrease of the Ni (848 eV) line is observed with changes of slope at about the same deposition times. This manner of the adsorbate and substrate AES signal variation is characteristic of the layer-by-layer growth mode. The first break of the Ba AP-PH variation at 14 min represents the completion of the first physical layer of barium and corresponds to ∼0.75 ML coverage. The second break at 28 min is due to the formation of the second layer at ∼1.5 ML coverage. The same growth mode has been documented for Ba adsorption on the clean Ni(110) surface [32]. However, the decrease of the substrate signal at the beginning of the Ba adsorption shows a deviation from linearity. This delay of the Ni (848 eV) signal reduction is probably related to the 2 × 1 phase, since no such substrate signal intensity behavior was recorded for Ba adsorption on the oxidized Ni(110) surface (not shown). The oxygen atoms initially reconstructs the Ni(110) surface and the 2 × 1 phase has been interpreted by different proposed models, such as the 'missing row' [34] and the added row [35]. It is likely that the Ba adatoms on the O(2 × 1) phase lift the oxygen-induced reconstruction of the nickel surface through the Ba–O interaction, producing this deviation from linearity for the Ni (848 eV) signal decrease. This consideration is in agreement with LEED observations, which showed that the 2 × 1 symmetry disappeared even at the very low Ba coverage (∼0.1 ML). The corresponding oxygen coverage in the O(2 × 1) phase has been previously reported to be 0.5 ML [36, 37]. The WF variation, $\Delta\Phi$, shown also in figure 1, is very similar to that of Ba growth on the clean nickel surface [32, 38]. This indicates that the Ba adatoms at the first layer become strongly positively polarized when reacting with the oxygen and/or the nickel atoms, while during the formation of the second layer (>0.75 ML) Ba approaches the metallic state due to the Ba–Ba interaction.

The low energy AES spectra for Ba adsorption on the O(2 × 1)/Ni(110) surface are shown in figure 2 for different barium coverages. The BaO (68 eV) line is attributed to an interatomic Auger transition involving the Ba 4d, Ba 5p and O 2p atomic levels, indicating the oxidation of Ba on the surface [39, 40]. On the other hand, the Ba (75 eV) line is due to a pure atomic transition related to the Ba 4d, Ba 5p and Ba 6s atomic levels [41]. Both of these lines are core–core–valence Auger transition lines and so they are very sensitive to the chemical changes on the surface induced by the oxidation of Ba. In fact, the intensity ratio of these lines helps to determine possible configurations of surface composition. Indeed, Haas *et al* have shown that the same amount of Ba and O atoms on W give different relative intensities of BaO (68 eV) and Ba (75 eV), depending on their particular atomic configuration [28]. It is noteworthy that while the Ba (75 eV) line is characteristic for pure Ba development on surfaces, it appears also for BaO growth on surfaces [40]. This can be explained by the adsorption of some Ba adatoms directly on Ni adsorption sites, with the O atoms not participating in the Ba–Ni interaction. Thus the first Ba layer seems to be partially oxidized.

As the barium overlayer grows on the oxygenated nickel surface, the lineshape of the AES spectra in the energy range below 60 eV changes dramatically. This is due to the developing Ba (57 eV) Auger transition line, which is overlapping with the Ni (61 eV) one. The substrate signal drastically decreases because of the masking effect. Above 60 eV, the BaO (68 eV) and Ba (75 eV) lines change too, with the intensity and the energy to be coverage-dependent. The energy shifts ΔE_1 and ΔE_2 of the BaO (68 eV) and Ba (75 eV) lines, respectively, are denoted in figure 2. Both lines move towards lower energies as the Ba coverage increases. We will discuss and analyze this effect in more detail later.

In figure 3 the AP-PH of the Ba (75 eV), BaO (68 eV) and O (510 eV) Auger transition lines are shown as a function of the barium deposition time. The Ba (75 eV) line increases until ∼14 min (0.75 ML), while the BaO (68 eV) one increases until ∼8 min (∼0.43 ML) and remains almost constant on further

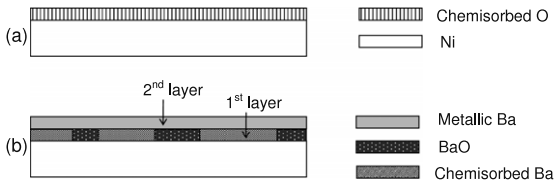

Figure 4. A simplified adsorption model for Ba deposition on the oxygenated O(2 × 1)/Ni(110) surface. (a) The oxygen chemisorbed nickel surface. (b) The interspersed by the chemisorbed Ba adatoms two-dimensional BaO layer (first layer) plus the metallic Ba overlayer (second layer).

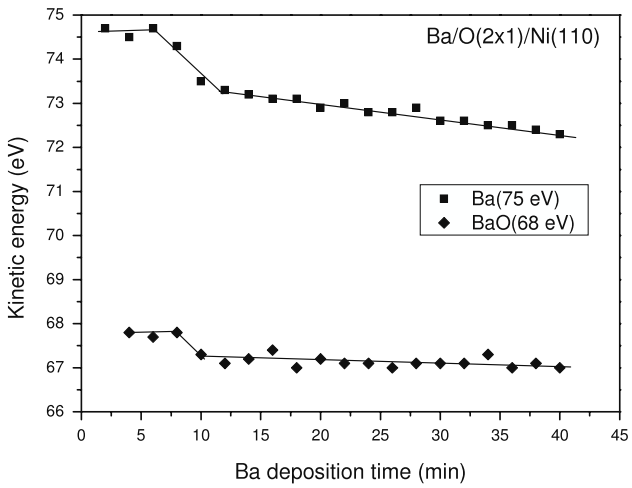

Figure 5. The energy of the Ba (75 eV) and BaO (68 eV) Auger transition lines as a function of the barium deposition time on the oxygen chemisorbed O(2 × 1)/Ni(110) surface.

deposition. The BaO (68 eV) line attests to the formation of BaO, which means that Ba reacts with the chemisorbed O atoms forming BaO during the growth of the first layer. Thus, according to the simplified electrostatic model, electrons move from the Ba 6s to the O 2p atomic orbitals. On the other hand, the O (510 eV) line shows a small initial increase up to about the time when the BaO (68 eV) line maximizes. This might be due to an 'upwards' movement of the chemisorbed O atoms reacting with the Ba ones forming BaO on the surface. This re-arrangement of the O atoms probably results in a de-reconstruction of the nickel surface, as manifested by the initial slower rate reduction of the Ni (848 eV) line observed in figure 1 and described above. When the BaO (68 eV) line stops increasing, we observe a more rapid increase of the Ba (75 eV) line up to ∼14 min. At this deposition time the first Ba layer is completed according to the results shown in figure 1. At the same time a decrease of the O (510 eV) line at an almost constant rate is observed as the Ba coverage increases. For a barium deposition time larger than 14 min, the Ba (75 eV) line does not increase substantially. This behavior can be attributed to the smaller escape depth of the Auger electron than the Ba overlayer thickness. The AP-PH variations in figure 3 indicate that the first layer of Ba consists of adatoms which interact with chemisorbed O atoms, forming an incomplete two-dimensional BaO layer. This BaO layer is interspersed by Ba adatoms interacting directly with Ni surface atoms. For coverage above 0.75 ML, Ba adatoms appear to interact with each other approaching the metallic phase as the characteristic WF curve shows (figure 1). According to this discussion, a simplified adsorption model is proposed and shown in figure 4. A similar adsorption model was suggested for the Ba adsorption on the preoxidized Ni surface, where Ba partially reduces the NiO substrate, forming an incomplete two-dimensional BaO layer confined between NiO and a metallic Ba overlayer [31].

As we mentioned above, both of the BaO (68 eV) and Ba (75 eV) Auger transition lines move towards lower energies as the Ba coverage increases. The energy of these lines is shown in figure 5 as a function of the Ba deposition time. We note that the energy of the Ba (75 eV) line displays a sudden decrease of ∼1.4 eV from 6 to 10 min, while at the same time the BaO (68 eV) line shows a corresponding small energy decrease by ∼0.5 eV. These AEES are similar to those measured when we studied Ba adsorption on an oxidized Ni(110) surface [31], and opposite to those observed for O adsorption on bariated nickel surfaces [42]. In the latter work the AEES were positive and bigger, with $\Delta E_K \sim 3$ eV for the Ba (75 eV) and $\Delta E_K \sim 2$ eV for the BaO (68 eV). This paradoxical behavior is probably due to the different process of developing BaO on the surface. In fact, here we develop BaO by adsorbing Ba on an oxygenated nickel surface, while in our previous work [42] we developed BaO by adsorbing O on bariated nickel surfaces. Different substrates define different chemical states or environments of the surface atoms, which means different initial state effects. According to our recent work [25], initial and final state effects play a decisive role in the energies of the atomic levels involved in the AES process. In the following, we analyze and discuss the observed AEES by combining our present AES results with previously performed photoemission measurements [25].

3.2. Correlation of the AES results with photoemission measurements

In principle, when the observed kinetic energy of an Auger electron changes, the energies of the three atomic levels involved may have changed too. This mostly happens when electron transfer takes place between the emitting atom and the environment, so the chemical state of the atom changes. Since the emitting atom is left doubly ionized, the surrounding electron distribution will affect the Auger energy (AE) too by a factor which is known as the extra-atomic relaxation energy. Also the change of the surface WF, $\Delta\Phi$, may affect the measured AE of the XYZ Auger electron in adsorption systems [25, 43]. Thus, we can write the following formula for the AE change, ΔE_K:

$$\Delta E_K = \Delta E_B(X) - \Delta E_B(Y) - \Delta E_B(Z) + \Delta R(Y,Z) - \Delta F(Y,Z) + a\Delta\Phi(\theta) \quad (1)$$

where $\Delta E(X)$, $\Delta E(Y)$ and $\Delta E(Z)$ are the binding energy shifts (BES) of the corresponding atomic levels of the Auger atomic transition, $\Delta R(Y,Z)$ is the change of the relaxation energy of the two holes left, $\Delta F(Y,Z)$ is the change of the electron–electron interaction, $\Delta\Phi$ is the work function change of the surface and a is a parameter which varies from 0 to 1, depending on the position of the emitting atom inside the

Table 1. The binding energy shifts of Ba and O core levels for a specific change of the Ba coverage (0.13 → 1.3 ML) on the oxygenated O(2 × 1)/Ni(110) surface.

$\Delta\theta$ (ML)	ΔE^*_B Ba(4d)	ΔE^*_B Ba(5p)	$\Delta E^*_B(V)$	ΔE^*_B O(2p)
0.13 → 1.3	0.8 eV	0.7 eV	1.5 eV	0.7 eV

induced surface dipole (0 when the atom is on the surface side, 1 when it is on the vacuum side) [43].

In a recent work, by using synchrotron radiation XPS measurements, we measured the BES, ΔE_B, of some atomic core levels for Ba adsorption on oxygen preadsorbed Ni(110) surface [25]. In the same work we also performed valence band measurements. Measuring both the ΔE_K and ΔE_B at the same Ba coverage eliminates the WF factor, $a\Delta\Phi(\theta)$, and equation (1) can be written

$$\Delta E_K = \Delta E^*_B(X) - \Delta E^*_B(Y) - \Delta E^*_B(Z) + \Delta R(Y,Z) - \Delta F(Y,Z) \quad (2)$$

where

$$\Delta E^*_B = \Delta E_B - a\Delta\Phi(\theta) \quad (3)$$

is the measured BES, corresponding to the WF change, $\Delta\Phi$. In table 1 we present the measured BES for core and valence band levels for Ba adsorption on the oxygenated O(2 × 1)/Ni(110) surface. It is worth noting that these are positive BES in contrast with previously reported negative BES for oxygen adsorption on barium pre-covered substrates [25].

Let us consider the Ba deposition on the chemisorbed O(2 × 1)/Ni(110) surface. Applying equation (2) for the Ba (75 eV) Auger transition line, we can write

$$\Delta E_K \text{ Ba (75 eV)} = \Delta E^*_B(4d) - \Delta E^*_B(5p) - \Delta E^*_B(V) + \Delta R(5p,V) - \Delta F(5p,V). \quad (4)$$

Taking into account the BES in table 1, we conclude that the first two terms in equation (4) increase the AE by 0.1 eV. So it is the last three terms that should account for the negative AE shift, $\Delta E_K = -1.8$ eV (figure 5). The chemisorbed Ba at 0.13 ML becomes progressively metallic at 1.3 ML. In our previous work [38], we have concluded that the Ba 6s level of the chemisorbed Ba adatoms on a nickel surface hybridizes with the initially empty 5d which becomes partially populated. The 5d 6s hybrid interacts with the Ni 3d orbitals, producing an emission feature at about ∼1.7 eV. When Ba becomes metallic a new emission appears at ∼4.7 eV due to the 6sp orbital hybridization [38]. The transition from the chemisorbed to the metallic state results in a positive $\Delta E^*_B(V)$ 1.5 eV [31]. Also, the $\Delta F(5p,V)$ is expected to be negative since the 5p states interact less strongly with the 6sp ones (metallic Ba), than with the more localized and spatially closer 5d states (chemisorbed Ba). Therefore, the $-\Delta F(5p,V)$ term in equation (4) should be positive, resulting in

$$\Delta R(5p,V) - \Delta F(5p,V) = -0.4 \text{ eV}. \quad (5)$$

So the conclusion for the extra-atomic relaxation energy change is $\Delta R(5p,V) < -0.4$ eV. This result is rather unexpected because, on going from the chemisorbed state of Ba adatoms to the metallic one, the relaxation energy should increase since the free electron density increases too. However, in the chemisorbed state a fraction of the Ba adatoms interacts with O, forming BaO with the easily polarizable O^{2-} anions increasing the relaxation energy. In addition, the surrounding Ni metal atoms contribute to the relaxation energy too. On the other hand, in the metallic phase (>0.75 ML), the relaxation energy comes not only from the underlying O^{2-} anions (first layer) but also from the surrounding Ba adatoms (second layer in figure 4). Since the density of states at the Fermi level of the metallic Ba is much lower than that of the metallic Ni (almost four times), the extra-atomic relaxation energy $R(5p,V)$ is plausible to decrease as the system goes from the chemisorption state to the metallic one. This might be a reasonable explanation for the resulting negative $\Delta R(5p,V)$. A similar extra-atomic relaxation energy decrease, $\Delta R(5p,V) < -0.6$ eV, was estimated for Ba adsorption on the oxidized Ni(110) surface [31].

In the same manner, working for the BaO (68 eV) Auger transition line we take

$$\Delta E_K \text{ BaO (68 eV)} = \Delta E^*_B(4d) - \Delta E^*_B(5p) - \Delta E^*_B(2p) + \Delta R(5p,2p) - \Delta F(5p,2p). \quad (6)$$

From figure 5, corresponding to the Ba coverage change (0.13 → 1.3 ML) measured, ΔE_K BaO (68 eV) is about −0.5 eV. The $\Delta F(5p,2p)$ can be considered equal to zero since it describes the change in the unscreened interaction between a Ba 5p electron and an O 2p electron. Thus, taking into account the values in table 1, we calculate the extra-atomic relaxation energy change, $\Delta R(5p,2p) = 0.1$ eV. This positive change is relatively small and within the experimental error, so we cannot extract safe conclusions studying the AEES of the BaO (68 eV) transition line.

4. Conclusions

In this work we studied the Ba adsorption on the O(2 × 1)/Ni(110) chemisorbed surface. The study was mainly based on the analysis of AES and WF results in combination with previous synchrotron radiation photoemission measurements. We conclude that, as the first physical layer of barium starts developing, the Ba adatoms interact with the chemisorbed O atoms forming a two-dimensional BaO layer, which is interspersed by Ba adatoms directly interacting with the nickel substrate. When the second layer of Ba begins to grow, the adsorbate approaches the metallic phase. During this transition, the low energy Auger lines of Ba (75 eV) and BaO (68 eV) shift towards lower energies with Ba coverage. The analysis showed that, for the Ba (75 eV) negative energy shift to have occurred, a decrease in extra-atomic relaxation energy is necessary, despite the fact that the final state is metallic barium. It is therefore concluded that the highly polarizable O^{2-} anions, coupled with the considerable reduction of the density of states at the Fermi level from Ni to metallic Ba, are responsible for this effect.

Acknowledgments

This work was in part financially supported by the European Community—Access to Research Infrastructure Action of the

Improving Human Potential Program (ARI). The authors thank Stefan Wiklund (Max-lab, Lund University) and the Max-lab National Swedish Institute for providing the facilities to perform the synchrotron radiation measurements.

References

[1] Franchy R 2000 *Surf. Sci. Rep.* **38** 195
[2] Renaud G 1998 *Surf. Sci. Rep.* **32** 1
[3] Henry C R 1998 *Surf. Sci. Rep.* **31** 231
[4] Tsami A, Grillo F, Bowker M and Nix R M 2006 *Surf. Sci.* **600** 3403
[5] Dow J D and Harshman D R 2007 *Int. J. Mod. Phys.* B **21** 3086
[6] Gaertner C and den Engelsen D 2005 *Appl. Surf. Sci.* **251** 24 and references therein
[7] Shih A, Yater J E and Hor C 2005 *Appl. Surf. Sci.* **242** 35 and references therein
[8] Matsumoto S 1996 *Catal. Today* **29** 43
[9] Stone P, Ishii M and Bowker M 2003 *Surf. Sci.* **537** 179
[10] Kim D H, Chin Y H, Kwak J H and Peden C H F 2008 *Catal. Lett.* **124** 39
[11] Desikusumastuti A, Laurin M, Happel M, Qin Z, Shaikhutdinov S and Libuda J 2008 *Catal. Lett.* **121** 311
[12] Van Doveren H and Verhoeven J A T 1980 *J. Electron Spectrosc. Relat. Phenom.* **21** 265
[13] Lampert W V, Rachocki K D, Lamartine B C and Haas T W 1982 *J. Electron Spectrosc. Relat. Phenom.* **26** 133
[14] Jacobi K, Astaldi C, Frick B and Geng P 1987 *Phys. Rev.* B **36** 3079
[15] Hill D M, Meyer H M III and Weaver J H 1990 *Surf. Sci.* **225** 63
[16] Vasquez R P 1991 *J. Electron Spectrosc. Relat. Phenom.* **56** 217
[17] Ozesnoy E, Peden C H F and Szanyi J 2006 *J. Phys. Chem.* B **110** 17001
[18] Hong I-H, Cheng C-P and Pi T-W 2007 *Surf. Sci.* **601** 1726
[19] Hong I-H, Cheng C-P and Pi T-W 2007 *Phys. Rev.* B **75** 165412
[20] Hwang C C, An K S, Park R J, Kim J S, Lee J B, Park C Y, Lee S B, Kimura A and Kakizaki A 1998 *J. Electron Spectrosc. Relat. Phenom.* **88–91** 733
[21] Hrbek J, Yang Y W and Rodriguez J A 1993 *Surf. Sci.* **296** 164
[22] Wertheim G K 1980 *J. Electron Spectrosc. Relat. Phenom.* **34** 309
[23] Bagus P S, Pacchioni G, Sousa C, Minerva T and Parmigiani F 1992 *Chem. Phys. Lett.* **196** 641
[24] Sousa C, Minerva T, Pacchioni G, Bagus P S and Parmigiani F 1993 *J. Electron Spectrosc. Relat. Phenom.* **63** 189
[25] Vlachos D, Kamaratos M and Foulias S D 2006 *J. Phys.: Condens. Matter* **18** 6997
[26] Haas G A, Shih A, Mueller D and Thomas R E 1992 *Appl. Surf. Sci.* **59** 227
[27] Bowker M, Stone P, Smith R, Fourre E, Ishii M and de Leeuw N H 2006 *Surf. Sci.* **600** 1973
[28] Haas G A, Thomas R E, Shih A and Marrian C R K 1989 *Appl. Surf. Sci.* **40** 265
[29] Mueller D and Shih A 1988 *J. Vac. Sci. Technol.* A **6** 1067
[30] Mueller D, Kurtz R L, Stockbauer R L, Madey T E and Shih A 1990 *Surf. Sci.* **237** 72
[31] Vlachos D, Foulias S D and Kamaratos M 2008 *Synth. React. Inorg. Met.-Org. Nano-Met. Chem.* **38** 400
[32] Vlachos D, Foulias S D, Kennou S, Pappas C and Papageorgopoulos C 1995 *Surf. Sci.* **331–333** 673
[33] Benndorf C, Egert B, Nöbl C, Seidel H and Thieme F 1980 *Surf. Sci.* **92** 636
[34] Smeenk R G, Tromp R M and Saris F W 1981 *Surf. Sci.* **107** 429
[35] Eierdal L, Besenbacher F, Laegsgaard E and Stensgaard I 1994 *Surf. Sci.* **312** 31
[36] Norton P R, Bindner P E and Jackman T E 1986 *Surf. Sci.* **175** 313
[37] Yagi-Watanabe K, Ikeda Y, Ishii Y, Inokuchi T and Fukutani H 2001 *Surf. Sci.* **482–485** 128
[38] Kamaratos M, Vlachos D and Foulias S D 2005 *Surf. Rev. Lett.* **12** 721
[39] Haas G A, Shih A and Marrian C R K 1985 *Appl. Surf. Sci.* **24** 447
[40] Haas G A and Shih A 1988 *Appl. Surf. Sci.* **31** 239
[41] Haas G A, Marrian C R K and Shih A 1983 *Appl. Surf. Sci.* **16** 125
[42] Vlachos D, Panagiotides N and Foulias S D 2003 *J. Phys.: Condens. Matter* **15** 8195
[43] Egelhoff W F Jr 1987 *Surf. Sci. Rep.* **6** 253